Biomass Conversion and Biorefinery (2022) 12:5959–5973
https://doi.org/10.1007/s13399-020-00996-4

ORIGINAL ARTICLE

Response of hydrolysis, methanogenesis, and microbial community structure to iron dose during anaerobic digestion of food waste leachate

Philip Antwi[1,2] · Dachao Zhang[1] · Wuhui Luo[1] · Felix Tetteh Kabutey[3] · Jianzheng Li[3] · Hao Su[1] · Meng Wu[1] · Zuwen Liu[1]

Received: 7 July 2020 / Revised: 25 August 2020 / Accepted: 2 September 2020 / Published online: 7 September 2020

Abstract

Anaerobic digestion (AD) of biodegradable organics depends heavily diverse functional genera, but an attempt to simultaneously enhance the various AD phases including the rate-limiting step (hydrolysis acidification) and methanogenesis has often remained a challenge. Although zero-valent iron (ZVI) supplementation had been proposed by many, its effect on the biomethanation process and microbial community evolution has not been fully explored. In this study, the response of hydrolysis acidification, methanogenesis, kinetics, pollutant removal efficiency, and microbial community evolution to various doses of ZVI employed in AD of food waste leachate was investigated and reported. When 10 g/L ZVI was dosed in the AD system, hydrolysis acidification, COD removal, biomethanation, and methane percentage were elevated by 18.9%, 67%, 39%, and 36%, respectively, as opposed to the control reactor (R1). Kinetics (R^2 of 0.998) revealed shorter lag phase (= 4.18 days) in ZVI-dosed reactors in contrast to longer periods (6.54 days) in R1. Methane production rate constant (k), sludge activity, and methane production rate estimated were 0.066 (day^{-1}), 0.83 gCH_4/gVSS, and 64.20 $mLCH_4$/gVSS/day, respectively, suggesting ZVI promoted methane production rate. Hydrolytic and methanogenic phyla including Firmicutes, Chloroflexi, Bacteroidetes, and Euryarchaeota were more enriched in ZVI-dosed reactors as opposed to R1. Acetoclastic-(*Methanosaeta*) and hydrogenotrophic-(*Methanobacterium*) methanogens were the most abundant genera of the archaea within ZVI-dosed assays, indicating acetoclastic methanogenesis was the main pathway.

Keywords Biochemical methane potential · Iron · Methane · Microbial community analysis · Anaerobic digestion

1 Introduction

As energy demand has increased exponentially in recent years, a significant number of concerns have been raised seeking to establish stringent policies on energy usage in order to curb its associated environmental pollution [27]. Therefore, the use of renewable energy as a potential substitute to supplement the global energy demand is currently being promoted extensively by many countries across the world [23]. Consequently, several strategies have been proposed, developed, and explored to enhance green energy (methane) production from biodegradable organics (biomass or organic carbon-rich wastewater) via anaerobic digestion (AD) [23, 27]. Methane generation from the AD of biodegradable organics has been one of the main pathways and this has substantially motivated many industries and municipal authorities to treat their biodegradable waste (solid or liquid) [29]. However, since AD involves complex microbial consortia including hydrolytic, acidogenic, syntrophic, acetogenic bacteria and methanogenic archaea to perform various functions at a given time, reducing conditions are required within the AD system in order to achieve optimum efficiency [10, 13, 28].

✉ Philip Antwi
kobbyjean@yahoo.co.uk

[1] School of Resources and Environmental Engineering, Jiangxi University of Science and Technology, Ganzhou 341000, Jiangxi Province, People's Republic of China

[2] School of Civil and Electrical Engineering, University of Southern Queensland, Darling Heights, Toowoomba, QLD 4350, Australia

[3] School of Municipal and Environmental Engineering, State Key Laboratory of Urban Water Resource and Environment, Harbin Institute of Technology, 73 Huanghe Road, Harbin 150090, People's Republic of China

Against this background, most research conducted in recent times have skewed significantly towards developing and implementing cost-efficient strategies and techniques that could enhance biogas or methane production during the AD process. Till date, a substantial number of substrate pretreatment methods including physical (thermal, ultrasonic, and microwave), chemical (alkaline and acidic), and mechanical treatment have been widely proposed and explored to elevate methane generation capacities and process kinetics within AD systems [17]. Although increment in methane production was achieved with these pretreatment methods, the extra methane generated could not compensate for the cost of the extra energy invested [5]. Therefore, exogenous additives or metal catalyst such as zero-valent metals (ZVM) into AD systems has been proposed in recent years, and this becomes a promising option due to its availability and low cost. ZVM addition to AD of organics has been explored, and notable performance has been demonstrated without any significant adverse effect [41]. For instance, zero-valent iron (ZVI) having a standard reduction potential ($Eh°$) of − 0.44 V is abundantly available, cheap to acquire, and can decrease oxidative-reductive potential (ORP) of the AD system to provide a conducive anaerobic environment for the anaerobes to perform efficiently [21].

Reducing oxidation (redox) potential has been established as a significant factor that improves the hydrolysis of the biodegradable proportion in the biomass or wastewater [22, 24, 31, 32]. Earlier reports have established that iron (ZVI) is a cofactor with a significant number enzymatic activity which typically occurs during acidogenesis. It has been further established that conductive iron oxides from ZVI are connected to the electron transfer between organic-oxidizing bacteria and methanogens [41]. As a result, activities of acetoclastic and hydrogenotrophic methanogens are enhanced by the electron donated from ZVI via corrosion [34]. ZVI under aquatic anaerobic conditions could enhance H_2 production (Eq. (1)) [43] that is mostly utilized by hydrogenotrophic methanogens as an electron donor for the reduction of CO_2 to CH_4 (Eq. (2)) [29]. It is also established that ZVI could stimulate acidogenic activities for the production of acetic acid that can be utilized by acetoclastic methanogens for the generation of CH_4 and CO_2 within the anaerobic oxidation pathways (Eq. (3)) [16, 29].

$$Fe° + 2H_2O \rightarrow Fe^2 + + H_2 + 2OH^- \quad (1)$$

$$4H_2 + CO_2 \rightarrow CH_4 + 2H_2O \quad (2)$$

$$CH_3COO^- + H^+ \rightarrow CH_4 + CO_2 \quad (3)$$

Puyol and coworkers had discussed that ZVI enhanced propionate fermentation activity and thus regulated propionate concentration which subsequently improved methanogenic activities [29]. Other earlier reports have also suggested that the introduction of Fe and its associate oxides could enrich Fe^{3+}-reducing microorganisms that can utilize a wide array of organics or substrates and thus participating in the biodegradation of complex polymers [6]. Although published reports have revealed that ZVI employed in most AD processes significantly improved methane yield, the optimum dose of the ZVI required has however not been fully explored to ascertain the dosage needed to optimize the AD system for optimum efficiency. Other research gaps that need to be addressed include identifying which dosages of ZVI that would tend to inhibit methanogens or affect the AD process adversely. Also, the response of microbial community evolution and process kinetic [37] to the various dosages of ZVI employed in AD also needs to be addressed through extensive studies. So far, the biological mechanisms involved in the ZVI systems are still unclear.

In this study, the effects of various doses of zero-valent iron (ZVI) on the rate-limiting hydrolysis acidification step, biomethane potential, microbial community evolution, process kinetics, and the related biological mechanisms were investigated. Thus, various ZVI doses were explored to (1) ascertain its contribution of effect on the hydrolysis acidification and biomethane potential from food waste leachate (FWL), (2) evaluate the effect of ZVI dose on the microbial community structure using 16S rRNA high-throughput gene sequencing, and (3) establish kinetics associated with AD supported by ZVI.

2 Materials and methods

2.1 Characteristics of food waste leachate, ZVI, and inoculum

Food waste leachate (FWL) was collected from a nearby food processing factory and stored in a refrigerator (SFMC-546C, Qingdao Smad Electric Appliances Co., Ltd., China) under 4 °C. The characteristics of the raw FWL were as follows: pH, 5.0 (subsequently adjusted to average pH of 7.2 using $NaHCO_3$); total chemical oxygen demand (TCOD), 25600 mg/L; total organic carbon (TOC), 4831 mg/L; ammonium (NH_4^+-N), 284 mg/L; total Kjeldahl nitrogen (TKN), 923 mg/L; total nitrogen (TN), 1239 mg/L; total suspended solids (TSS), 19921 mg/L; volatile suspended solids (VSS), 13800 mg/L; and alkalinity (ALK), 3825 mg/L. FWL was diluted to a suitable concentration and supplied into batch reactors (Table 1).

Carbon to nitrogen (C/N) ratio of the FWL was 20.01, an indication that the estimated C/N ratio had corroborated with the theoretical C/N ratio (20–30) for anaerobic digestion [26]. Zero-valent iron ($Fe°$) powder (surface area, diameter, and purity of 0.05 m^2/g, 0.2 mm and > 98%, respectively) was added into batch assays (Table 1). Anaerobic granule sludge collected from a lab scale mesophilic UASB treating piggery

Table 1 Physicochemical characteristics of diluted FWL, inoculum, and rector condition

Parameter	Mean	Reactors				
		R1	R2	R3	R4	R5
Quality of diluted FWL						
TCOD (mg/L)	1180					
NH_4^+-N (mg/L)	96					
pH (mg/L)	7.2					
ALK (mg $CaCO_3$/L)	2945					
tVFAs (mg/L)	201					
Protein (mg/L)	822					
Carbohydrate (mg/L)	1334					
FWL-TSS (g/L)	4.63					
FWL-VSS (g/L)	2.6					
Characteristics of sludge						
Inoculum MLSS (g/L)	4.24					
Inoculum MLVSS (g/L)	2.11					
Initial condition in reactors						
F/M ratio		0.56	0.56	0.56	0.56	0.56
ZVI dosage (g/L)		0	1	5	10	15

wastewater was used as inoculum in the batch assays. The mixed liquor suspended solids (MLSS) and mixed liquor volatile suspended solids (MLVSS) of the granule sludge determined as directed in the standard methods [4] were 4.24 g/L and 2.11 g/L, respectively.

2.2 Analytical methods

All physical and chemical parameters (total chemical oxygen demand (TCOD), soluble chemical oxygen demand (SCOD), alkalinity (ALK—in terms of $CaCO_3$), ammonium (NH_4^+-N), ferrous iron (Fe^{2+}), total phosphorus (TP), MLSS, and MLVSS) were determined in accordance with protocols established in standard methods [4]. NH_4^+-N, Fe^{2+}, and TP were measured using UV spectrophotometer (Shimadzu, UV-VIS, Japan). pH was determined with a precision ion meter (Zhengzhou Nanbei Instrument Equipment Co., Ltd., PXS-450). Shandong Lunan Instrument gas chromatograph (model SP6890) was employed to determine specific VFAs and their corresponding concentrations within the AD batch reactors. In this study, nitrogen gas was employed as the carrier gas under the column head pressure of 0.75 MPa. Working temperatures of the oven, detector, and the injection port of the gas chromatograph were 210 °C, 180 °C, and 210 °C, respectively. Biogas produced within batch reactors was measured with a lubricated syringe. To determine specific gases and their corresponding proportions within the produced biogas, another gas chromatograph (SP-6800A, manufactured by Shandong Lunan Instrument) with detector, oven, and injection port temperatures set at 80 °C, 50 °C, and 80 °C, respectively, was employed herein. Thus, 0.5 ml of the biogas produced was sampled from the headspace of every batch reactor and injecting into the gas chromatograph to establish percentages of gas fractions. Protein and carbohydrate were determined by the protocol described by Zhao and coworkers [42].

2.3 Batch experiments

2.3.1 Hydrolysis-acidification (experiment I)

In experiment I, the influence or impact of ZVI on the hydrolysis acidification efficiency of organics within the FWL was evaluated. 2-Bromoethanesulfonic acid (BESA) (50 μM) was added into each serum bottle inoculated with anaerobic sludge to inhibit and prevent methanogens from oxidizing VFAs during hydrolysis-acidification step [8]. Obtained anaerobic sludge from a lab scale UASB was washed severally with 0.1 M PBS before using it to inoculate each batch reactor. Next, ZVI powder of 1, 5, 10, and 15 g/L was added into batch assays R2, R3, R4, and R5, respectively. All batch assays (R1, R2, R3, R4, and R5) were capped with rubber stoppers, flushed with N_2 gas for 3–5 min, and kept in a 35 °C mechanical shaker (YK-3102, Dong Guan Yaoke Instrument Equipment Co., Ltd) swirling at 140 revs/min. The accumulated VFAs were measured after a 3-day fermentation period.

2.3.2 Influence of ZVI on biomethanation (experiment II)

It has been reported that biomethanation is conducted via digestion of acetate or H_2/CO_2 by acetoclastic and hydrogenotrophic methanogens, respectively [12]. Therefore, the effect of ZVI on methanogens (acetotrophic and hydrogenotrophic) could be employed to assay their influence on syntrophic methane production. In this study, digestion of FWL with and without ZVI was conducted in 150-ml serum bottles having an effective working volume of 100 ml (Table 1). After inoculum (anaerobic sludge obtained from an UASB) and FWL were added into the serum bottles, all batch reactors (R1, R2, R3, R4, and R5) had a final concentration of 1.18 g/L (Table 1). ZVI was subsequently added into each reactor at dosages of 0, 1, 5, 10, and 15 g/L in R1, R2, R3, R4, and R5, respectively. Endogenous biogas generation was also evaluated using blank assays (inoculum added into deionized water) to establish whether inoculum could generate some in situ gases. Biochemical methane potential (BMP) analysis was conducted in duplicate, and the averaged values were presented. The food to microorganism ratio established in each reactor was about 0.56. Before incubation, each fermentation batch assay was purged with N_2 gas for 3–5 min and then sealed with butyl rubber stoppers to prevent gas escape. Assays were finally incubated in a shaking incubator

(YK-3102, Dong Guan Yaoke Instrument Equipment Co., Ltd) under 35 °C and swirling at a speed of 140 rev/min. The biogas production rate and composition were determined daily using lubricate syringes and gas chromatograph, respectively. pH and total COD in the effluent were determined at the end of the digestion period. In order to evaluate methane yield, mass balance estimations were performed for each reactor (Eqs. (4, 5, and 6)).

$$\text{Yield} = \text{accumulation in headspace of reactor} + \text{output} \quad (4)$$

$$Y = [(M_2 - M_1) \times V_h]_{\text{accumulation}} + \left[\frac{(M_1 + M_2)}{2} \times V_b\right]_{\text{output}} \quad (5)$$

$$Y_{\text{net}} = Y_{\text{reactor}} - Y_{\text{control}} \quad (6)$$

where Y is the methane generated (mL), Y_{reactor} is the methane generated in batch reactor (mL), Y_{control} is the methane generation in R1-control (mL), Y_{net} is the net methane generation in reactor (mL), M_1 is the initial methane percentage in biogas (%), M_2 is the final methane percentage in biogas (%), V_h is the volume of headspace (mL), and V_b is the volume of total biogas produced (mL).

2.4 Kinetic modeling and statistical analysis

2.4.1 Kinetic modeling

Methane yield from batch assays was modeled using kinetic models to fit on the curves. Five different kinetic models were engaged in non-linear kinetic modeling to evaluate methane production rate constant (k), sludge activity, methane potential (M_0), maximum methane production rate ($R_{\max}$), and lag phase ( ) using first-order exponential model, modified Gompertz model, transference function model, logistic function model, and Sigmoid function model in Eqs. (7), (8), (9), (10), and (11), respectively [24]. Besides the specific methane yield and the cumulative methane yield, the lag phase is a critical kinetics parameter and tends to explain or determine that the efficiency of the AD process was also thoroughly evaluated and discussed [40]. Herein, the lag phase ( ) was estimated with the logistic function model shown in Eq. (4) [40].

$$M(t) = M_0 \times \left(1 - e^{(-kt)}\right) \quad (7)$$

$$M(t) = M_0 \times \exp\left\{-\exp\left(\frac{R_{\max} \cdot e}{M_0}(\ -t) + 1\right)\right\} \quad (8)$$

$$M(t) = M_0\left\{1 - \exp\left(-\frac{R_{\max} \cdot (t-\ )}{M_0}\right)\right\} \quad (9)$$

$$M(t) = M_0 / \left\{1 + \exp\left(\frac{4 \cdot R_{\max} \cdot (\ -t)}{M_0} + 2\right)\right\} \quad (10)$$

$$M(t) = M_0 / \left\{1 + \exp - \left(\frac{R_{\max} \cdot e}{M_0}(\ -t) + 1\right)\right\} \quad (11)$$

where $M(t)$ is the cumulative methane yield (mL/gVSS added), M_0 is the methane potential of the substrate (mL/gVSS added), k is the methane production rate constant (1/day), is the lag phase (day), e is the Euler's function given by the absolute value of 2.7183, and t is the time (days).

2.4.2 Statistical analysis

Analysis of variance (ANOVA) was performed on results of methane production and organic pollutant (COD) removal by using Sigmaplot software (version 13.0) at 5% level of significance to know the differences between the treatments. All models employed in this study were incorporated into the Sigmaplot (version 12.5) platform to estimate the kinetics parameters and subsequently predicting methane yield. The models were validated with a coefficient of determination (R^2) (Eq. (12)) and [9] standard error of the estimates (SEE) (Eq. (13)) [7] in order to demonstrate goodness-of-fit of the proposed models [9].

$$R^2 = \frac{\sum_{i=1}^{n}\left(Y_p - \overline{Y}\right)^2}{\sum_{i=1}^{n}\left(Y_o - \overline{Y}\right)^2} \quad (12)$$

$$\text{SEE} = \sqrt{\frac{\sum_{i=1}^{n}\left(Y_o - Y_p\right)^2}{n-m}} \quad (13)$$

where Y_o, Y_p, $\overline{Y}$, n, and m denote experimental data, predicted values, arithmetic mean of the observed data, number of data points, and number of parameters in the regression model, respectively.

2.5 Microbial community structural analysis by 16S rRNA gene sequencing

Sludge samples including those in batch reactors (R1, R2, R3, R4, and R5) and inoculum (S_0) were analyzed for microbial community diversity. As performed in previous work, DNA Isolation Kit manufactured by MOBIO Laboratories, Inc., USA, was employed to extract total DNA from samples [2, 11]. The DNA extraction was followed by agarose gel electrophoresis to check the integrity and concentration of genomic DNA [14]. Subsequently, genomic DNA was quantified for PCR reaction. Samples of genomic DNA were amplified with universal primers ((341F) 5′-CCTACGGGAGGCAG CAG-3′ and (805R) 5′-GACTACHVGGGTATCTAATCC-3) which spanned the V3–V4 hypervariable region of the 16S rRNA gene [18, 19]. Next, PCR amplification was performed to a final volume of 50 μL which specifically contained 10 ng of the genomic DNA, 0.5 μL dNTP

(10 mM each), 0.5 μL of each PCR primer (50 μM), and 0.5 μL of Taq (5 U/μL). Eppendorf Mastercycler was employed to perform PCR amplification under the conditions detailed in our previous work [2]. After PCR amplification, agarose gel electrophoresis was conducted to retrieve DNA PCR products separation [39]. Amplified products were again analyzed in agarose gel (1%) before sequencing. DNA was finally sequenced with high-throughput approach on Illumina Miseq sequencing platform (Sangon Biotech Shanghai Co. Ltd, China). FLASH software (version 1.2.7) was employed to merge all paired-ends reads. Quality controlling including barcode and primer trimming, chimera checking, and filtering of sequence reads containing homo-polymer stretches was conducted based on barcode sequence of each sample. PRINSEQ software (PRINSEQ-lite 0.19.5) was used to remove primer, short, and poor-quality sequences among reads from samples. Uchime software removed chimeric sequences and Uclust software (version 1.1.579) for sequence alignment.

3 Results and discussion

3.1 Effect of ZVI on the hydrolysis acidification step: mechanisms and efficiency

It has been well established that complex polymers (organic matter) cannot be directly utilized for methanogenesis until it is converted to CO_2, or VFA (acetate, propionate, etc.) or formates [41]. Therefore, to evaluate the effect of ZVI on the solubilization of TCOD during the AD process, the hydrolysis acidification phase was investigated and illustrated in Figs. 1 and 2. The evolution of volatile fatty acids and its related specific metabolites was determined and used to evaluate the hydrolysis acidification efficiency during AD of FWL. ZVI doses of 1, 5, 10, and 15 g/L were introduced into batch mode AD reactors after methanogenic activities within the inoculum had been inhibited with BESA. The fermentation process lasted for 3 days after which residual total COD and related anaerobic metabolite (VFAs) in the effluent were determined (Figs. 1, 2, and Table 2). At the end of the 3-day fermentation, it was found that ZVI in batch reactors had effectively promoted COD hydrolysis and acidification (total VFAs (TVFAs)) efficiency as opposed to that in control reactor (R1-no ZVI added) (Fig. 1 and Table 1). Consequently, TVFA concentrations increased from an initial value of 201.4 mg/L in the control reactor (R1) to 2391, 2459, 2628, 2699, 2841 mg/L in R2, R3, R4, and R5, respectively. The remarkable performance of ZVI-dosed reactors in terms of hydrolysis was attributed to the presence of obligate anaerobes which attained its optimum workability at a more negative ORP promoted by ZVI [3, 21].

The results suggested TVFAs had increased by 2.7%, 9.9%, 12.8%, and 18.9% in R2, R3, R4, and R5, respectively, as opposed to the R1 (Fig. 1). This result corroborated with previous reports where ZVI was added into AD and hydrolysis was measured with protease and α-glucosidase activities. It was reported that protease and α-glucosidase activities increased by 26% and 8% in ZVI-dosed reactors as opposed to the control [34]. In another study conducted by Feng and coworkers where sludge was digested anaerobically with ZVI, it was reported that the activities of key enzymes in hydrolysis acidification increased from 0.6 to 1 as opposed to the control reactor [13]. This remarkable observation made in this present study suggested that ZVI addition in proper dosages could effectively and rapidly accelerate the rate-limiting step of hydrolysis acidification during AD digestion. It was also noticeable that results obtained in R3 and R4 were not significant likewise R4 and R5. The predominant metabolites determined within the TVFA body were acetate followed by propionate, iso-butyrate, and butyrate (Fig. 2). Averaged acetate concentration measured was 1120, 1277, 1573, 1769, and 1902 mg/L in R1, R2, R3, R4, and R5, respectively, representing about 14.01%, 40.44%, 57.94%, and 69.82% of acetate increase in R2, R3, R4, and R5, respectively. It is worthwhile mentioning that the production of acetate revealed in this study was approximately 1.69-fold increase compared to the control reactor. A similar observation was made by Vyrides and coworkers who reported on improved hydrolysis in waste-activated sludge using Fe_3O_4. On this note, it was concluded that ZVI addition could enhance hydrolysis acidification particularly acetate production which is one principal metabolite necessary for optimum methane yield at the methanogenesis step.

Although maximum acetate production was realized in R5 where 15 g/L ZVI was added, the difference concerning that in 10 g/L was minimal and not significant. Propionate concentrations, however, decreased along with increasing ZVI additions (Fig. 2). As revealed in other reports, acetic-type, propionic-type, and butyric-type fermentation are the three major fermenting pathways in AD process [3]. However, propionic-type fermentation is reported as a facultative anaerobic process occurring at an ORP higher than − 278 mV, while acetic-type and butyric-type fermentation are obligate anaerobes which attain its optimum workability at a more negative ORP [3]. Other reports had confirmed that iron (Fe) could promote electron donor process and thereby reducing CO_2 into CH_4 through autotrophic methanogenesis [13]. Therefore, the results obtained herein suggested that ZVI which is a reductive material proved its ability to enhance the AD process. This phenomenal observation which is in agreement with the assertion in made earlier reports might be one of the ideal justification for the increase in acetate and decrease in propionate (Fig. 2a), which however is a favorable condition for methanogenesis [13]. In summary, ZVI enhanced solubilization of organics significantly.

Table 2 Performance of batch reactors and estimated methane yield by kinetic models

Reactor	Measured CH_4 (mL/gVSS)	CH_4 fraction (%)	Effluent total COD (mg/L)	Total COD removal (%)	Residual TVFA in effluent (mg/L)	Effluent pH
R1	384 ± 0.3	52.9 ± 0.1	352.2	70.15	312 ± 0.6	7.3
R2	490 ± 0.5	58.0 ± 0.2	217.6	81.56	256 ± 1.2	7.6
R3	576 ± 0.1	63.6 ± 0.6	149.4	87.34	198 ± 0.9	7.7
R4	642 ± 0.6	71.8 ± 0.8	29.5	97.51	82 ± 0.8	7.9
R5	589 ± 0.8	66.8 ± 0.4	102.8	91.29	213 ± 1.1	7.6

3.2 Effect of ZVI on the biomethanation and pollutant removal process: mechanisms, efficiency, and application

Earlier reports have established that ZVM such as ZVI could elevate methane production from bio-organics via anaerobic digestion [34, 41]. As a result, the effect of ZVI on the BMP and kinetics was evaluated during AD of FWL using another set of batch assays (Tables 2 and 3). The study revealed that ZVI had significantly promoted FWL during the anaerobic digestion process and the mechanisms involved corroborated with other reports [20]. After 20 days of digestion (Fig. 3a and Table 2), it was found that ZVI had positively influenced biogas production, methane production, and pollutant removal process in all ZVI-dosed reactors as opposed to the control reactor. This further suggested that no inhibitory factor(s) were present to affect the AD process (Table 2). At the commencement of each run, methane and daily biogas yield in each reactor had increased until it attained a maximal around day 15. As illustrated and presented in Fig. 3a and Table 2, the cumulative methane yield in R1, R2, R3, R4, and R5 was 382.8, 489.7, 576.4, 642.1, and 589.4 $mLCH_4$/gVSS, respectively, an indication that ZVI-dosed reactors had increased methane production by 27.93%, 50.57%, 67.74%, and 53.97%, in R2, R3, R4, and R5, respectively, as opposed to the R1. Notably, R4 with 10 g/L ZVI dose recorded the highest net methane yield and TCOD removal of 642.1 $mLCH_4$/gVSS and 97.5%, respectively (Table 2).

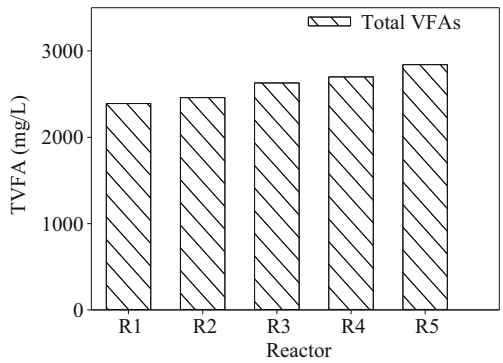

Fig. 1 Effect of ZVI dose on total volatile fatty acid production after 3 days of fermentation

The remarkable performance observed in ZVI-dosed reactors were attributed to ZVI addition. Thus, ZVI was believed to have (i) enhanced electrons donor process, (ii) promoted activities of hydrolysis acidification enzymes, (iii) significantly decrease ORP within the AD system and subsequently providing favorable environment for anaerobes to perform well, and (iv) enhanced growth among acetogens and hydrogenotrophic methanogens to consume acetate and H_2, respectively, for a smooth drive of the digestion process. Figure 3a, b, and microbial community analysis further suggested that the acetoclastic and hydrogenotrophic methanogenesis pathways were the main metabolic pathways during methanogenesis. Considering the lower residual acetate in the effluent and significant production of methane in the ZVI-dosed reactors, it was believed that acetoclastic methanogenesis (methanation from in situ produced acetate) had occurred and was feasible due to the extra electrons donated by the ZVI besides (CO). Again, hydrogenotrophic methanogenesis pathway was also feasible as some hydrogenotrophic genera belonging to the archaea were observed this study (Table 4). In response, it was revealed that CH_4 production via H_2/CO_2 had occurred in reactors with ZVI dosage as a lower concentration of H_2/CO_2 was recorded in biogas fractions but rather, higher methane yield compared to the control (R1) (Fig. 3a and Table 2).

The overall observation revealed that ZVI had a significant effect on the hydrolysis acidification processes and had promoted acetoclastic methanogenesis better compared with hydrogenotrophic methanogenesis. The consumption of hydrolysis acidification products within the enhanced methanogenesis system might have driven hydrolysis acidification forward via thermodynamics. Thus, the hydrolysis process in ZVI-dosed reactor was not inhibited and was consistently achieved as a result of the addition of ZVI. This superficial occurrence originated from the increased

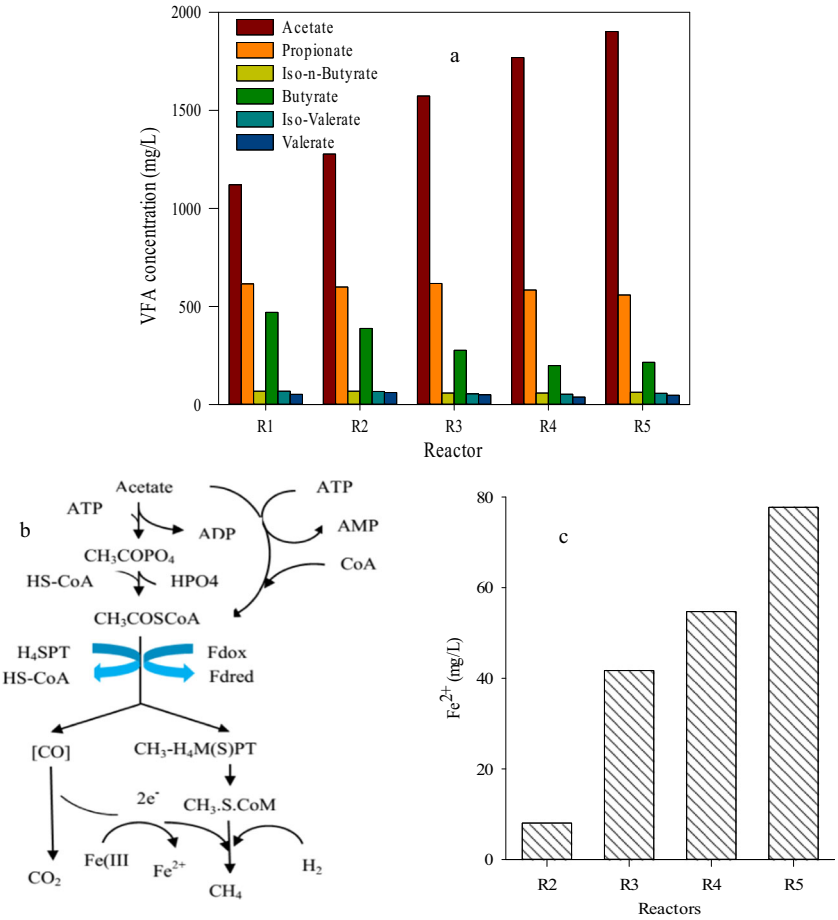

Fig. 2 Effect of ZVI on hydrolysis acidification and methanogenesis: **a** volatile fatty acid profile after 3-day fermentation, **b** pathway of biomethanation from in situ production of acetate, **c** evolution of Fe^{2+} after 3-day fermentation

methanogenesis activity that subsequently utilized the hydrolytic metabolites to promote hydrolysis acidogenesis. The observation observed herein concurred with another published report where a novel zero-valent iron (ZVI) technology to enhance anaerobic methane production from primary sludge was studied [36]. In that study, reactors with ZVI doses of 1, 4, and 20 g/L played a symbolic role in the methane production compared to the control. Thus, BMP of about 439 L CH_4/kgVS was achieved in ZVI-dosed reactor whereas only 345 L CH_4/kgVS was observable in the control reactor [36]. Methane generation from syntrophic metabolism was also feasible as established by Zhao and coworkers [41]. In that study, Zhao had suggested that the promotion of syntrophic metabolism between syntrophic bacteria and methanogens by ZVI was feasible and hence that could have contributed to the high methane production observed in their study [41]. Therefore, the significant improvement in methane yield observed in ZVI-dosed reactors in this study concurred to and had a strong correlation with the assumptions made by Zhao and coworkers. It was also worth noting that the fraction of methane in the biogas was also affected by ZVI dosage. Methane percentages in produced biogas were highest in ZVI-dosed reactors (58–71.8%) compared with the control reactor (52.9%). Again, the highest methane proportion was observed in R4 where ZVI of 10 g/L was employed. On the other hand, it was observed that methane yield and percentages in R5 (15 g/L) had decreased compared with those in R4, indicating ZVI optimum dose could be around 10 g/L and that higher doses could adversely affect the AD process (Table 2).

Regarding pollutant removal process, it was found that TCOD removal in R1, R2, R3, and R5 was 70.1%, 81.56%, 87.3%, and 91.2%, respectively, indicating TCOD removal had increased in ZVI-dosed reactors by 16–39% compared with the blank reactor. Noticeably, the performance of ZVI-induced reactors dominated R1 (without ZVI) regarding pollutant removal. These observations further affirmed previous facts and proved that ZVI contributed to the biodegradability of FWL. Within anaerobic environments, ZVI could be oxidized by water into ferrous ions (Eq. (1)) to facilitate the generation of H_2, and this leads to higher CH_4 yield as H_2 is converted into methane via hydrogenotrophic methanogenesis (Eq. (2)).

The direct generation of H_2 from ZVI corrosion within non-oxidative environments has been proposed as a mechanism for the enhanced methanation [15]. Although ZVI addition for enhanced methanation is justifiable following its significant contribution to methane production, it is however not enough justification to conclude on to employ ZVI at full scale

Table 3 Results from batch assays and kinetic modeling (95% confidence interval)

Kinetic parameters	Batch reactors				
	R1 (control)	R2	R3	R4	R5
ZVI added (g/L)	0	1	5	10	15
BMP measured (mL/gVSS)	384 ± 0.3	490 ± 0.5	576 ± 0.1	642 ± 0.6	589 ± 0.8
CH_4-COD (g/L)	1.07 ± 0.1	1.24 ± 0.6	1.62 ± 0.1	1.77 ± 0.3	1.59 ± 0.7
COD_{fed} (g/L)	1.14 ± 0.4	1.36 ± 0.1	1.71 ± 0.8	1.82 ± 0.5	1.66 ± 0.5
Biomethane potential (μ_b)	0.94 ± 0.9	0.91 ± 0.7	0.95 ± 0.9	0.97 ± 0.4	0.96 ± 0.1
Sludge activity (g CH_4-COD/g VSS)	0.51 ± 0.5	0.58 ± 0.4	0.77 ± 0.3	0.83 ± 0.7	0.75 ± 0.2
First-order kinetic mode					
k (day^{-1})	0.018	0.033	0.041	0.066	0.048
R-squared	0.883	0.889	0.925	0.955	0.921
BMP predicted (mL/gVSS)	422.6	552.3	634.1	700.1	667.5
Modified Gompertz model					
(day)	6.24	5.62	4.46	4.20	4.19
R_{max} (mL/gVSS·days)	54.68	66.68	57.98	59.15	64.23
R-squared (R^2)	0.991	0.988	0.995	0.995	0.991
BMP predicted (mL/gVSS)	393.2	506.1	597.6	684.25	615.2
Transference function model					
(day)	8.83	7.57	6.39	6.30	6.28
R_{max} (mL/gVSS·days)	29.85	41.42	44.59	47.15	49.47
R-squared (R^2)	0.921	0.932	0.961	0.972	0.950
BMP predicted (mL/gVSS)	442.14	556.12	632.15	715.69	660.9
Logistic function model					
(day)	6.54	5.95	5.06	4.18	4.72
R_{max} (mL/gVSS·days)	56.38	69.08	62.58	64.20	68.66
R-squared (R^2)	0.998	0.996	0.998	0.997	0.997
BMP predicted (mL/gVSS)	390.16	495.86	571.87	655.63	599.70
Sigmoid function model					
(day)	10.01	9.51	7.21	5.24	5.15
R_{max} (mL/gVSS·days)	1.73	1.77	1.82	1.97	1.89
R-squared (R^2)	0.989	0.975	0.991	0.989	0.984
BMP predicted (mL/gVSS)	393.12	499.47	579.01	669.67	607.44

as Fe^{2+} could bind preferentially with some other anions such as HCO_3^-/CO_3^{2-} and SH^-/S^{2-} and subsequently precipitate to form other salts [29]. Based on the latter assertions, it is possible to conclude that ZVI for enhanced methanation is not economically and environmentally viable and that ZVI addition in anaerobic digestion of organic waste/water treatment requires extensive research to prove its economic and environmental viability at both lab and full-scale capacities. In this study, Fe^{2+} production increased (8.02, 41.71, 54.72, and 77.75 mg/L in R2, R3, R4, and R5) along with increasing ZVI dose. However, a similar observation was made and reported by Feng and coworkers and went further to suggest that Fe^{2+} produced in the reaction had no major significant influence on the methanation [13]. Although the latter report mentioned little contribution by ZVI addition per methane production, this study, however, realized remarkable and enhanced methane production in ZVI dose reactors during AD of FWL (Fig. 3). The observation made herein suggested that Fe^{2+} was released as ZVI contributed to the electron donor process to promote methanogenesis activity. Besides our observation, enhancement of methane production was also reported earlier when ZVI was added into anaerobic digestion [38].

3.3 Process kinetics study of methane production

3.3.1 Simulation of methane production for selecting optimum kinetic models

To further establish the effect of ZVI on AD of FWL, methane production was simulated with kinetic models in order evaluate kinetic parameters that are of the utmost importance when one seeks to address or describes an AD process. Cumulative

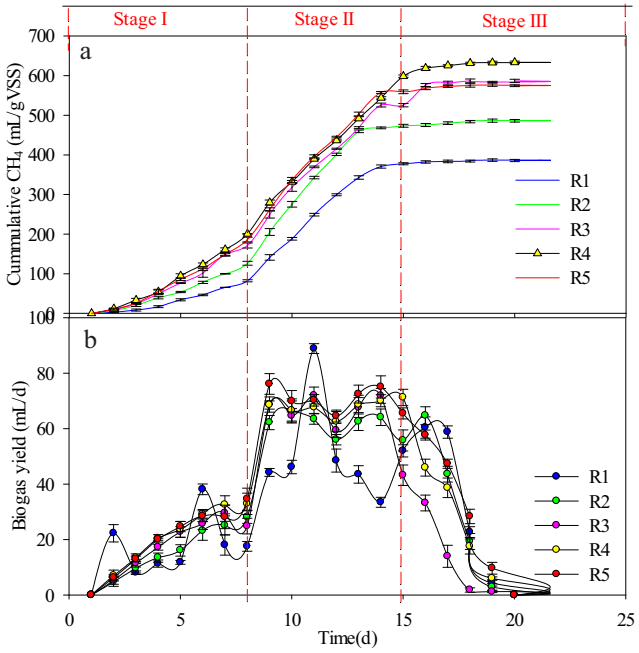

Fig. 3 Time course of methane production in batch reactors: **a** cumulative methane and **b** daily biogas yield

methane production data observed in control reactor (R1) and ZVI-dosed reactors were subsequently simulated using five different kinetic models, *viz*. first-order model, modified Gompertz model, modified logistic model, transference model, and sigmoid model. Kinetics parameters including methane potential, lag phase, and methane production rate were evaluated using batch experiment data (Table 3). The performance output of the modified logistic model was much satisfactory followed by modified Gompertz and sigmoid model.

Within the batch mode AD of FWL, the proposed models particularly modified logistic and modified Gompertz models estimated the kinetic parameters on the assumption that growth rate (GR) of the bacteria specifically the archaea methanogens in the inoculum was proportional to the gas produced; these gas productions exhibited sigmoidal curves [1]. Among the test runs (R1, R2, R3, R4, and R5), the predicted methane yield (M(t)) estimated by the transference function model and first-order model was significantly higher than that measured from experiments. This observation revealed the inefficiencies of the models (transference function and first order) to replicate methane production data. In a study conducted by Li and coworkers, it was mentioned that transference model is mostly employed where there is almost or close to zero lag phase time. In that situation, the model works better by considering the stationary and exponential phase in the biogas production [24].

Notably, all five models predicted an increase in methane production rate and decreased in lag phase time with an increase in ZVI dosage (Table 3). Consequently, a remarkable performance was put up by logistic function compared to the modified Gompertz model, sigmoid function model, and transference function models. In comparison to other works, similar efficiencies of the model were established when the same models were employed to predict methane production from thermally pretreated lignocellulose waste material [33]. In their study, it was revealed that modified Gompertz model predictions agreed well with the experimental results followed by modified logistic and transference models, which is somehow in harmony with the observation made in this present study [33]. In order to evaluate the soundness and efficiency of the proposed logistic function model, visual agreements and correlations of the predicted values (methane yield) and cumulative net methane productions were plotted (Fig. 4).

It was is found that the coefficient of determination (R^2) observed in Fig. 4b, d, f, h, and j ranged between 0.996 and 0.998. The logistic model output fitted well to the experimental results in R1 and R4 (R^2 = 0.998) as opposed to R2, R3, and R5 whose R^2 were 0.996, 0.997, and 0.997, respectively.

3.3.2 Methane production rate constant (*k*) and lag phase time (*λ*)

Table 3 presents *k* values estimated with the first-order model which ranged between 0.018 and 0.066 day^{-1} in all the experiments. Observably, ZVI introduced into the AD process had

Table 4 Operational taxonomic units, estimated diversity, richness indices for inoculum, and batch reactors sludge

Sample	OTUs	Richness indices		Diversity indices		Good's sampling coverage
		ACE estimator	Chao1 estimator	Shannon diversity	Simpsons inverse	
sSo	3867	2887.69	23013.07	5.33	0.03	0.95
sR1	3194	2895.72	23884.60	4.42	0.05	0.97
sR2	3287	2968.24	22543.94	4.18	0.02	0.97
sR3	3568	3004.38	26389.35	4.31	0.04	0.96
sR4	3057	2789.32	18962.68	4.29	0.04	0.97
sR5	3119	2667.59	17926.23	4.12	0.05	0.96

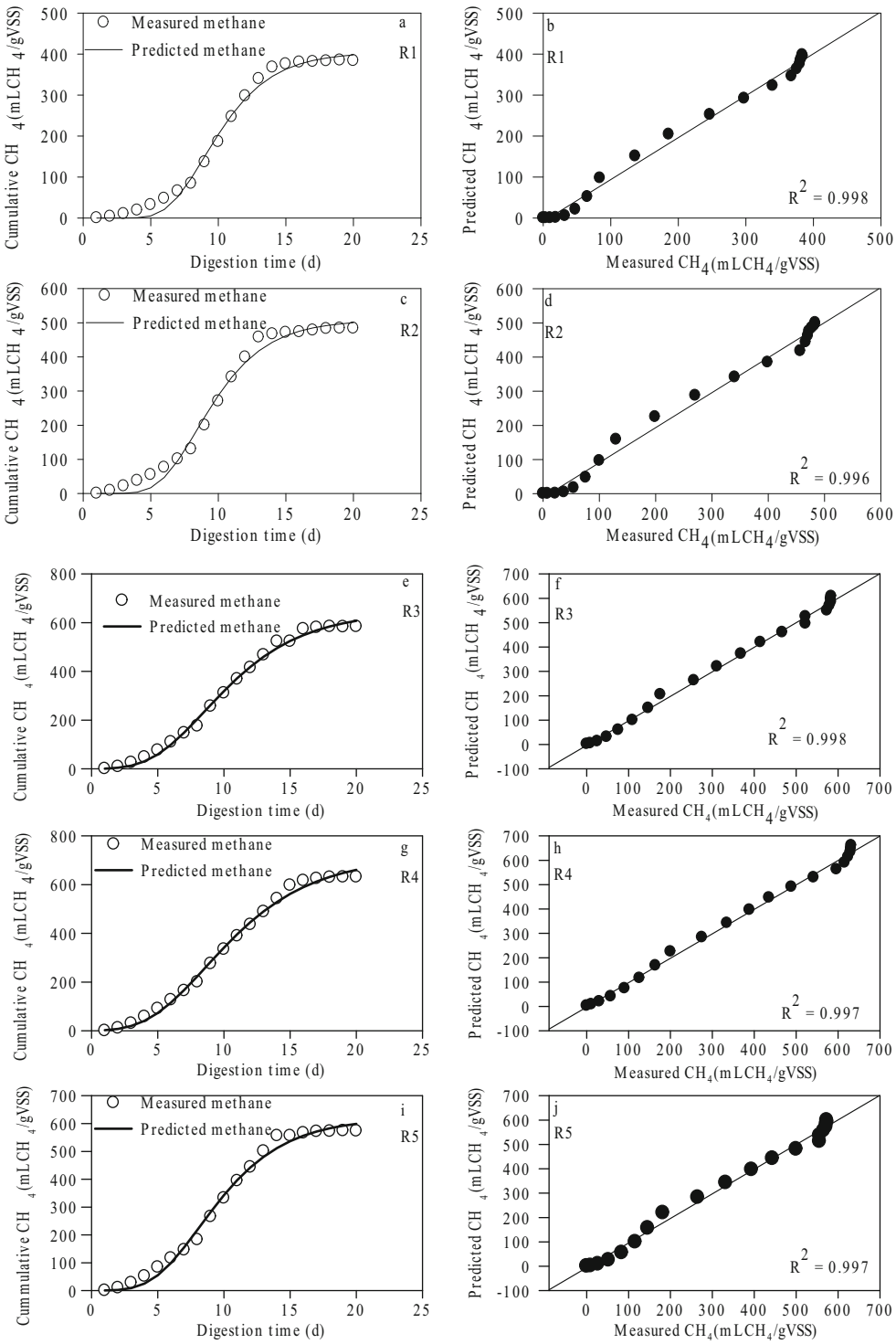

Fig. 4 Logistic model predictions and measured BMP: visual agreements (**a**, **c**, **e**, **g**, **i**); correlations (**b**, **d**, **f**, **j**, **h**)

significantly influenced the rate constant (k) concerning the various ZVI doses (control, 1, 5, 10, and 15 g/L) employed. It was observed that reactors with maximum methane production as opposed to the control reactor (R1) had relatively higher k values ranging between 0.033 and 0.066 day^{-1}. The highest k value of 0.066 day^{-1} was recorded in R4 with 10 g/L ZVI whereas the least was recorded in R1 with a k value of 0.018 day^{-1}. In this observation, it was established that the addition of ZVI into the AD of FWL could facilitate hydrolysis, acidification, acetogenesis, and methanogenesis step. Therefore, the observed increase in biogas and methane production in the ZVI-based reactor is attributable to the ZVI addition as opposed to reactors without ZVI. While highest k value (0.066 day^{-1}) observed was affiliated to R4 (Table 3), it

further suggests that optimum performance of the AD process could be achieved when ZVI dose of 10 g/L is employed for anaerobic bio-transformation of organics into methane. To further appreciate the potential effect of ZVI on the AD process of FWL, Fig. 5 was constructed to further illustrate the effect on the hydrolysis rate (k) and the biomethane potential (M_0). In Fig. 5, it was observable that both k and M_0 moved rightward and upward, suggesting the effect of ZVI on the k and M_0 as opposed to non-ZVI-based reactor (R1). On the overall, the results obtained in this study went contrary to those observed in Liu and coworkers' report where they indicated that ZVI addition had no significant effect on degradation rate coefficient (k) values (0.083 day^{-1}, 0.072 day^{-1}) per observation made in two different experiments [25]. However, this work has manifested that ZVI additions could impact on the methane production process.

Logistic function model predicted a shorter lag phase period ( ) of 4.18 days when 10 g/L ZVI into added into R4 digesting FWL under mesophilic condition. On the other hand, R1 without ZVI recorded a longer lag phase time of 6.54 days. The corresponding coefficient of determination (R^2) values of the logistic function model while predicting methane production data in the control reactor (R1) and ZVI-dosed reactors ranged 0.996–0.998. The prolonged lag phase observed in R1 which corresponded to the low biogas production rate could be blamed on the residual organics (protein and carbohydrate) that required sufficient time to undergo AD.

3.3.3 Biochemical methane potential (*μb*) and sludge activity

Biological degradation of organic pollutant could be expressed as biochemical methane potential (μb) [3]. Therefore, COD conversion into CH_4 denoted as BMP (μb) is another parameter to evaluate the efficiency of the experiment in this study. In this study, it was revealed that 20 days was the average time to achieve maximum μb with FWL and anaerobic sludge as inoculum. Therefore, the results of BMP

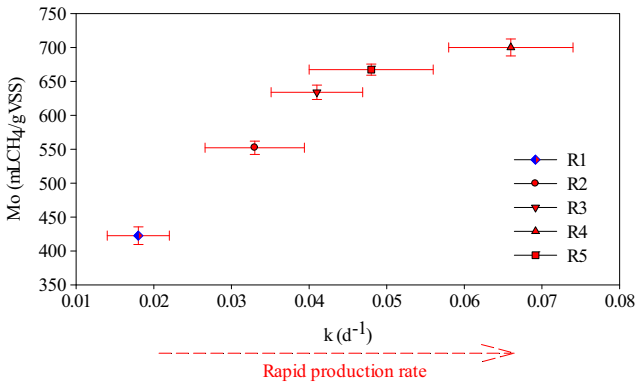

Fig. 5 Plot of hydrolysis rate (k [day^{-1}]) and biochemical methane potential (M_0, $mLCH_4/gVSS$) of FWL digested under the anaerobic condition with and without ZVI addition

(μb) as summarized in Table 3 were recorded after 20 days and indicated as $μb_{20}$. In Table 3, it was evident that maximum BMP (μb) of 0.97 $gCH_4/gCOD$ fed was obtained in R4 followed by R3 and R5. The observation thus appears to be consistent with the methane production rate constant (k) estimated and presented in Table 3. The trend in the results further suggests that without ZVI or low concentrations of ZVI will yield minimum μb as observed in R1 and R2 with μb of 0.94 and 0.91 $gCH_4/gCOD$ fed, respectively. Notably, CH_4 production appeared affected by the dose of ZVI as ZVI < 1 g/L or > 10 g/L adversely affects or reduces μb. Therefore, it could be deduced that the optimal dose of ZVI required to produce a significant volume of methane during FWL digestion was 10 g/L followed by 5 g/L.

To determine the quality of sludge and how fast it could convert substrate to methane (methanogenic activity), it is of utmost importance to determine the sludge activity of the given inoculum. Also, an application of this methanogenic testing (sludge activity) could also help to establish the toxic effect that specific wastewater exerts on an anaerobic sludge. By ascertaining sludge characteristics (sludge-activity (SA)), an added advantage is gained forehand during the selection of an adapted sludge to be used in an anaerobic digester [26]. Thus, determination of sludge activity is a valuable exercise to help identify potentially unfavorable conditions among a consortium of microorganisms. In this study, therefore, sludge activity measurement was evaluated and presented in Table 3. Compared with R1, R2, R3, and R5, maximum sludge activity of 0.83 g CH_4/g VSS was recorded in R4 (Table 3). Considering μb value ≥ 0.95 $gCH_4/gCOD$fed as 100% sludge activity [26], it goes to suggest that, sludge activity in R3, R4, and R5 was 100% whereas that in R1 and R2 was 98% and 95%, respectively.

3.4 Diversity and taxonomic classification of the microbial communities

Statistical analysis of sequences obtained from 16S rRNA high-throughput gene sequencing is presented in Table 4. As presented in Table 4, the observed OTUs associated with all six samples (S_o, R1, R2, R3, R4, and R5) ranged 3057 to 3867. Compared to the inoculum, lower OTUs in sludge obtained from batch assays observed indicating richness had decreased during the BMP. This reduction in OUT was more pronounce when ZVI of 10 g/L was employed. Shannon and Chao1 indices estimated reduced from 5.33 in the inoculum (S_o) to a range of about 4.12 to 4.42 of the sludge obtained from the batch reactors. The latter observation suggested that bacterial diversity had changed in batch assay mainly when ZVI was introduced (Table 4). The efficiency of the molecular analysis was estimated with Good's coverage, richness, and diversity (Table 4).

Dynamics in the microbial community at the phylum level was investigated and illustrated in Fig. 6. The high-throughput sequencing methodology revealed a total of 37 phyla among which Chloroflexi, Firmicutes, Euryarchaeota, Bacteroidetes, Synergistetes, Proteobacteria, Caldiserica, Spirochaetes, Actinobacteria, and Thermotogae were observed as the most dominant in all six samples (S_o, R1, R2, R3, R4, and R5). In order to establish the effect of ZVI on the microbial community dynamics, the community structure of the sludge obtained from the control reactor (R1) was compared with sludge obtained from the ZVI-dosed reactors. The inoculum (S_o) was dominated with Firmicutes (20.36%) followed by Synergistetes (17.12%), Proteobacteria (14.35%), Bacteroidetes (14.34%), Chloroflexi (11.35%), and Euryarchaeota (9.01%). The dominance of these phyla within the inoculum was believed to have driven the hydrolysis acidification and methanogenesis process within the batch assays [3]. Microbial community succession in R1 (at the phylum level) was significantly different from reactors dosed with ZVI (Fig. 6). It was found that Firmicutes population had increased by 96.8% in R3 when compared to the inoculum whereas only 78.3% increase was observed with R1. Chloroflexi population, a major hydrolytic bacterium had reduced in all batch assays except R4 which saw a subtle growth (Fig. 6). Chloroflexi population was maintained ZVI-based reactors but reduced in R1 significantly by 24.8%. The low performance associated with R1 as opposed to R2, R3, R4, and R5 were attributable to the presence of a higher abundance of hydrolytic bacteria including Firmicutes and Chloroflexi. However, Bacteroidetes, Proteobacteria, and Synergistetes which also possess hydrolysis and acetogenesis functionalities [14] were reduced in all batch assays (Fig. 6). Conversely, Euryarchaeota, which is one of the four phyla of archaea, was observed to have increased in population with increase ZVI dose. With the introduction of 1 g/L ZVI (R2), Chloroflexi (22.34%) dominated the community structure followed by Firmicutes (18.74%), Euryarchaeota (13.99%), Bacteroidetes (13.54%), Synergistetes (10.23%), and Proteobacteria (8.54%). Notably, these major phyla observed in R2 had decreased in population except Chloroflexi and Euryarchaeota, an indication that ZVI addition had maintained their existence.

In R3 dominant phyla included Chloroflexi (24.97%), followed by Firmicutes (18.25%), Euryarchaeota (15.24%), Bacteroidetes (11.32%), Synergistetes (8.74%), and Proteobacteria (7.95%) whereas R4 was Chloroflexi (24.68%), Euryarchaeota (22.68%), Firmicutes (20.54%), Proteobacteria (9.87%), Synergistetes (8.21%), and Bacteroidetes (5.64%). Similarly, all dominant phyla decreased in population except Chloroflexi and Euryarchaeota which encountered growth instead (Fig. 6). However, when 15 g/L ZVI was dosed in R5, the dominant phyla were Euryarchaeota (21.68%) followed by Chloroflexi (18.74%), Firmicutes (16.42%), Proteobacteria (11.30%), Synergistetes (9.87%), and Bacteroidetes (8.64%). The observation

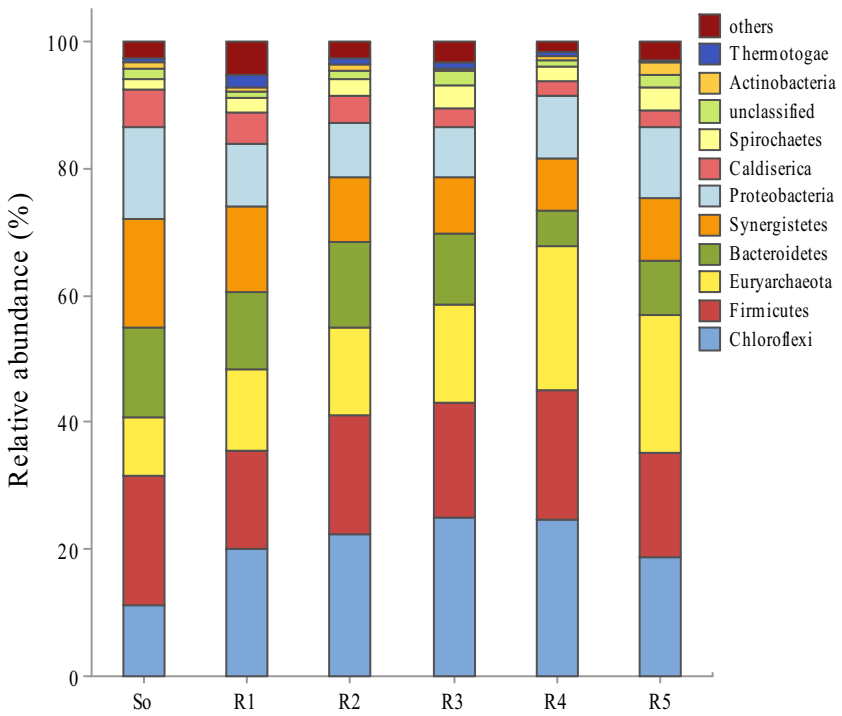

Fig. 6 Relative abundance of microbial communities at the phylum level (phylum < 1% of the total sequences were reported as "others") in the inoculum (So) and batch reactors (R1, R2, R3, R4, and R5)

affirmed that ZVI contributed significantly to the community dynamics by increasing Euryarchaeota and Chloroflexi population that was, however, necessary for the methanation process. On the contrary, the results observed R5 demonstrated that cell damage relative to the higher dose of ZVI was feasible [37].

At the genus level, the relative abundances of genera and unclassified sequences were reported (Fig. 7). Genera belonging to Euryarchaeota were predominantly acetoclastic (*Methanosaeta*) and hydrogenotrophic (*Methanobacterium*) methanogens. Compared with the inoculum, genus *Methanosaeta* increased by 26.0%, 54.8%, 63.0%, 171.2%, and 205.5% in R1, R2, R3, R4, and R5 (Fig. 7). Thus, *Methanosaeta* increased 2.71- and 3.1-fold in R4 and R5 compared with R1 with only 1.2-fold. As both genera (*Methanosaeta* and *Methanobacterium*) are reported to be mostly affiliated with biogas digesters [35], it suggested that the enhanced methane production observed in the ZVI-dosed reactors (methane production increased by 27.93%, 50.57%, 67.74%, and 53.97%, in R2, R3, R4, and R5, respectively) had a strong correlation between the abundance of *Methanosaeta* and *Methanobacterium* genera as opposed to R1. Although *Methanosaeta* was found to be more pronounced in the ZVI-dosed reactors, it was deduced that this genus was tolerant to inhibition present in the acetoclastic pathway system as they are often more tolerant of specific inhibitors of the [30]. The observation made herein suggested that Fe^{2+} was released and contributed to the electron donor process.

Genus	So	R1	R2	R3	R4	R5
Methanosaeta	7.3	9.2	11.3	11.9	19.8	22.3
Unclassified	19.3	13.2	12.3	10.2	13.4	14.7
Levilinea	5.2	10.2	12.1	15.4	14.4	10.2
Thermovirga	16.6	15.2	11.0	6.4	5.3	4.7
Longilinea	5.8	4.2	7.2	9.5	7.1	6.0
Caldisericum	8.3	8.1	6.3	4.9	4.6	3.6
Syntrophomona	2.2	3.2	5.2	6.9	3.5	6.4
Ethanoligenens	4.9	3.5	5.1	2.9	3.1	3.6
Exilispira	2.8	3.5	3.8	4.9	3.3	3.0
Leptolinea	3.3	3.7	4.2	3.8	3.3	2.5
Alkaliflexus	3.8	2.7	4.0	2.9	2.9	3.3
Desulfovibrio	1.6	4.2	1.3	2.3	2.9	3.3
Clostridium XI	0.3	0.7	1.0	2.2	2.5	0.1
Azospira	1.1	0.6	0.6	0.3	0.5	1.1
Clostridium sensu stricto	1.2	0.2	0.3	1.7	0.4	0.7
Smithella	0.4	0.4	0.3	0.4	1.9	0.3
Clostridium IV	0.4	0.6	0.5	0.2	0.6	0.3
Phascolarctobacterium	0.2	1.3	0.4	0.1	0.1	0.3
Parabacteroides	1.3	1.1	1.6	0.2	0.2	0.2
Aminobacterium	0.6	0.3	0.2	0.2	0.4	0.2
Methanobacterium	0.2	0.2	0.5	0.3	0.1	0.4
Bacteroides	0.0	0.3	0.5	0.6	0.4	0.5
others	13.2	13.3	10.3	11.5	10.2	13.2

Fig. 7 Heatmap showing relative abundances of genera (where sequence reads considered in at least one sample was ≥ 1%) observed in batch reactors

4 Conclusion

This study illuminated the effects of ZVI on the biomethanation, mechanism, and microbial community succession during AD of food waste leachate. ZVI addition impacted positively on the AD process as hydrolysis acidification efficiency, pollutant removal efficiency, biomethane-potential (BMP), and methane proportions. Methane proportions increased by 18.9%, 67%, 39% (642.1 $mLCH_4/gVSS$), and 36% when 10 g/L ZVI was employed (R4) as opposed to the control reactor (R1). Kinetic modeling (R^2 of 0.998) revealed shorter lag phase (=4.18 days) in ZVI reactors (R4) as opposed to longer periods (6.54 days) observed in R1, an indication that ZVI dose of 10 g/L as the optimum dosage for the AD process. Within ZVI reactors, particularly R4 and R5, acetoclastic (*Methanosaeta*) and hydrogenotrophic (*Methanobacterium*) methanogens were the predominant members of archaea at the genus level, suggesting acetoclastic methanogenesis was the main pathway to have been heavily promoted by the ZVI addition. It was also found that hydrolytic phyla such as Firmicutes, Chloroflexi, and Bacteroidetes were more pronounced in ZVI-dosed reactors. The mechanisms observed in this study provided potential theoretical basis to depend on in the quest to initiate a full-scale implementation of biomethane generation via ZVI-based AD system.

Funding This research was funded by the Natural Science Foundation of Jiangxi Province, China (Grant Number 20202BAB203019), the Scientific Research Start-up Fund of Jiangxi University Science and Technology-China (Grant Number JXXJBS18033), and the National Natural Science Foundation of China (Grant Number 51464014). The authors are much grateful to these institutions and all individuals who contributed to the success of this research.

References

1. Altaş L (2009) Inhibitory effect of heavy metals on methane-producing anaerobic granular sludge. J Hazard Mater 162(2-3): 1551–1556
2. Antwi P, Li J, Boadi PO, Meng J, Quashie FK, Wang X, Ren N, Buelna G (2017a) Efficiency of an upflow anaerobic sludge blanket reactor treating potato starch processing wastewater and related process kinetics, functional microbial community and sludge morphology. Bioresour Technol 239:105–116
3. Antwi P, Li J, Boadi PO, Meng J, Shi E, Xue C, Zhang Y, Ayivi F (2017b) Functional bacterial and archaeal diversity revealed by 16S rRNA gene pyrosequencing during potato starch processing wastewater treatment in an UASB. Bioresour Technol 235:348–357
4. Apha A (2005) WEF (2005) Standard methods for the examination of water and wastewater. Am Public Health Assoc Am Water Works Assoc Water Environ Fed
5. Ariunbaatar J, Panico A, Esposito G, Pirozzi F, Lens PN (2014) Pretreatment methods to enhance anaerobic digestion of organic solid waste. Appl Energy 123:143–156
6. Baek G, Kim J, Cho K, Bae H, Lee C (2015) The biostimulation of anaerobic digestion with (semi) conductive ferric oxides: their

potential for enhanced biomethanation. Appl Microbiol Biotechnol 99(23):10355–10366
7. Barampouti E, Mai S, Vlyssides A (2005) Dynamic modeling of biogas production in an UASB reactor for potato processing wastewater treatment. Chem Eng J 106:53–58
8. Basu S, Oleszkiewicz J, Sparling R (2005) Effect of sulfidogenic and methanogenic inhibitors on reductive dehalogenation of 2-chlorophenol. Environ Technol 26(12):1383–1392
9. Bhattarai S, Kim DH, Oh J-H (2012) Simulation and model validation of a pneumatic conveying drying for wood dust particles. J Biosyst Eng 37(2):82–89
10. Budych-Gorzna M, Smoczynski M, Oleskowicz-Popiel P (2016) Enhancement of biogas production at the municipal wastewater treatment plant by co-digestion with poultry industry waste. Appl Energy 161:387–394
11. Corbellini V, Kougias PG, Treu L, Bassani I, Malpei F, Angelidaki I (2018) Hybrid biogas upgrading in a two-stage thermophilic reactor. Energy Convers Manag 168:1–10
12. Dong B, Xia Z, Sun J, Dai X, Chen X, Ni B-J (2019) The inhibitory impacts of nano-graphene oxide on methane production from waste activated sludge in anaerobic digestion. Sci Total Environ 646: 1376–1384
13. Feng Y, Zhang Y, Quan X, Chen S (2014) Enhanced anaerobic digestion of waste activated sludge digestion by the addition of zero valent iron. Water Res 52:242–250
14. Fu S-F, Chen K-Q, Sun W-X, Zhu R, Zheng Y, Zou H (2018) Improved methane production of corn straw by the stimulation of calcium peroxide. Energy Convers Manag 164:36–41
15. Guan X, Sun Y, Qin H, Li J, Lo IM, He D, Dong H (2015) The limitations of applying zero-valent iron technology in contaminants sequestration and the corresponding countermeasures: the development in zero-valent iron technology in the last two decades (1994–2014). Water Res 75:224–248
16. Hao X, Wei J, van Loosdrecht MC, Cao D (2017) Analysing the mechanisms of sludge digestion enhanced by iron. Water Res 117: 58–67
17. Hashemi SS, Karimi K, Mirmohamadsadeghi S (2019) Hydrothermal pretreatment of safflower straw to enhance biogas production. Energy. 172:545–554
18. Herlemann DP, Labrenz M, Jürgens K, Bertilsson S, Waniek JJ, Andersson AF (2011) Transitions in bacterial communities along the 2000 km salinity gradient of the Baltic Sea. ISME J 5(10):1571–1579
19. Hugerth LW, Wefer HA, Lundin S, Jakobsson HE, Lindberg M, Rodin S, Engstrand L, Andersson AF (2014) DegePrime, a program for degenerate primer design for broad-taxonomic-range PCR in microbial ecology studies. Appl Environ Microbiol 80(16):5116–5123
20. Hwang Y, Sivagurunathan P, Lee M-K, Yun Y-M, Song Y-C, Kim D-H (2019) Enhanced hydrogen fermentation by zero valent iron addition. Int J Hydrog Energy 44(6):3387–3394
21. Jiang Z, Lv L, Zhang W, Du Q, Pan B, Yang L, Zhang Q (2011) Nitrate reduction using nanosized zero-valent iron supported by polystyrene resins: role of surface functional groups. Water Res 45(6):2191–2198
22. Junyapoon S (2005) Use of zero-valent iron for wastewater treatment. Kmitl Sci Tech J 5(3):587–595
23. Li W, Khalid H, Zhu Z, Zhang R, Liu G, Chen C, Thorin E (2018) Methane production through anaerobic digestion: participation and digestion characteristics of cellulose, hemicellulose and lignin. Appl Energy 226:1219–1228
24. Li L, Kong X, Yang F, Li D, Yuan Z, Sun Y (2012) Biogas production potential and kinetics of microwave and conventional thermal pretreatment of grass. Appl Biochem Biotechnol 166(5): 1183–1191
25. Liu Y, Wang Q, Zhang Y, Ni B-J (2015) Zero valent iron significantly enhances methane production from waste activated sludge by improving biochemical methane potential rather than hydrolysis rate. Sci Rep 5:8263
26. Negi S, Dhar H, Hussain A, Kumar S (2018) Biomethanation potential for co-digestion of municipal solid waste and rice straw: A batch study. Bioresour Technol 254:139–144
27. O'Shea R, Wall DM, Murphy JD (2017) An energy and greenhouse gas comparison of centralised biogas production with road haulage of pig slurry, and decentralised biogas production with biogas transportation in a low-pressure pipe network. Appl Energy 208:108–122
28. Park KY, Jang HM, Park M-R, Lee K, Kim D, Kim YM (2016) Combination of different substrates to improve anaerobic digestion of sewage sludge in a wastewater treatment plant. Int Biodeterior Biodegradation 109:73–77
29. Puyol D, Flores-Alsina X, Segura Y, Molina R, Padrino B, Fierro J, Gernaey KV, Melero JA, Martinez F (2018) Exploring the effects of ZVI addition on resource recovery in the anaerobic digestion process. Chem Eng J 335:703–711
30. Schnürer A, Nordberg Å (2008) Ammonia, a selective agent for methane production by syntrophic acetate oxidation at mesophilic temperature. Water Sci Technol 57(5):735–740
31. Sleiman N, Deluchat V, Wazne M, Mallet M, Courtin-Nomade A, Kazpard V, Baudu M (2016) Phosphate removal from aqueous solution using ZVI/sand bed reactor: Behavior and mechanism. Water Res 99:56–65
32. Velimirovic M, Schmid D, Wagner S, Micić V, von der Kammer F, Hofmann T (2016) Agar agar-stabilized milled zerovalent iron particles for in situ groundwater remediation. Sci Total Environ 563: 713–723
33. Vivekanand V, Mulat DG, Eijsink VG, Horn SJ (2018) Synergistic effects of anaerobic co-digestion of whey, manure and fish ensilage. Bioresour Technol 249:35–41
34. Vyrides I, Andronikou M, Kyprianou A, Modic A, Filippeti A, Yiakoumis C, Samanides CG (2018) CO2 conversion to CH4 using zero valent iron (ZVI) and anaerobic granular sludge: Optimum batch conditions and microbial pathways. J CO2 Util 27:415–422
35. Walter A, Silberberger S, Juárez MF-D, Insam H, Franke-Whittle IH (2016) Biomethane potential of industrial paper wastes and investigation of the methanogenic communities involved. Biotechnol Biofuels 9(1):21
36. Wei W, Cai Z, Fu J, Xie G-J, Li A, Zhou X, Ni B-J, Wang D, Wang Q (2018) Zero valent iron enhances methane production from primary sludge in anaerobic digestion. Chem Eng J 351:1159–1165
37. Wu D, Zheng S, Ding A, Sun G, Yang M (2015) Performance of a zero valent iron-based anaerobic system in swine wastewater treatment. J Hazard Mater 286:1–6
38. Yin Q, Yang S, Wang Z, Xing L, Wu G (2018) Clarifying electron transfer and metagenomic analysis of microbial community in the methane production process with the addition of ferroferric oxide. Chem Eng J 333:216–225
39. Yuan L, Qi A, Cheng Y, Sagen G, Qu Y, Liu B (2017) Fecal microbiota of three bactrian camels (Camelus ferus and Camelus bactrianus) in China by high throughput sequencing of the V3-V4 region of the 16S rRNA gene. J Arid Land 9(1):153–159
40. Zhang H, Zhang P, Ye J, Wu Y, Fang W, Gou X, Zeng G (2016) Improvement of methane production from rice straw with rumen fluid pretreatment: a feasibility study. Int Biodeterior Biodegradation 113:9–16

41. Zhao Z, Zhang Y, Li Y, Quan X, Zhao Z (2018) Comparing the mechanisms of ZVI and Fe3O4 for promoting waste-activated sludge digestion. Water Res 144:126–133
42. Zhao Z, Zhang Y, Quan X, Zhao H (2016) Evaluation on direct interspecies electron transfer in anaerobic sludge digestion of microbial electrolysis cell. Bioresour Technol 200:235–244
43. Zhen G, Lu X, Li Y-Y, Liu Y, Zhao Y (2015) Influence of zero valent scrap iron (ZVSI) supply on methane production from waste activated sludge. Chem Eng J 263:461–470